Effect of the Organometallic Fragment R = −CCHCo$_2$(CO)$_6$ on the Properties of M$_2${OOCR}$_4$ Clusters (M = Mo, Cu)

Víctor Calvo-Pérez,*,† Andrés Vega,†,‡ and Evgenia Spodine†

Facultad de Ciencias Químicas y Farmacéuticas, CIMAT, Universidad de Chile, Casilla 233, Santiago, Chile, and Universidad de Tarapacá, Av. General Velásquez 1775, Arica, Chile

Three structures of novel cluster carboxylates of molybdenum(II) (**1a**−**c**) and copper(II) (**2**) with the OOC−CCHCo$_2$(CO)$_6$ ligand are presented. The solvent topology plays an important role in the formation of the crystal lattice of the molybdenum(II) cluster, which shows a pillared structure for **1**, with stacked 1,4-xylene (**1a**,**b**) and toluene (**1c**). The nature of the cluster···solvent interaction has been investigated by means of B3LYP density functional theory calculations using double-ζ basis functions. These DFT calculations together with polarizable continuum media and effective fragment potentials allow us to explain the nature of the arene···Mo$_2$ arrangement (ca. 3.10 Å) found in the pillared cluster **1b**. The copper(II) dimer **2** displays an unexpected weak intramolecular magnetic coupling for a copper tetracarboxylate, which can also be ascribed to the electronic nature of the ligand. The weak coupling within the copper(II) *syn*,*syn*-carboxylate cluster was investigated with DFT calculations. In the solvated species the copper(II) cluster **2** presents an oxo ligand at the axial positions, while the molybdenum(II) cluster **1** stacks between the aromatic ligands.

Introduction

The assembly of heterometallic species using well-defined molecular building blocks is a very general approach for obtaining complex species, which has been shown to be very fruitful in many fields of chemistry.[1] In particular, a synthetic approach called cluster of clusters has shown to be very successful in producing compounds with new properties using well-described coordination chemistry. It consists of the use of functionalized organometallic clusters as building blocks, which can be coordinated to a core of metal atoms or cationic groups, acting as an anchoring point. The newly assembled compounds generally show properties which are not present in the inorganic analogues. Some of the most striking examples have been reported for the M$_2${OOCCCo$_3$(CO)$_9$}$_4$ (M = Mo, Cr, W) series, where a low-energy charge-transfer band is observed between both metallic subsystems (Mo, Cr, W, and Co) in contrast to the acetate analogues.[2,3]

We have recently prepared and characterized a new organocobalt carboxylic acid, HOOCCCHCo$_2$(CO)$_6$,[4] which has been employed to prepare new heterometallic compounds. The electronic structure of the Re$_2${OOCCCHCo$_2$(CO)$_6$}$_4$Cl$_2$ compound has been examined by means of cyclic voltammetry and DFT calculations.[5] The observed difference in the reduction potentials of the Re$_2$ and cobalt carbonyl fragments, in comparison to rhenium trimethyl acetate and HOOCCCHCo$_2$(CO)$_6$, has been attributed to the mixing of both subsystems in the assembled species.[5] In addition, the reactivity of HOOCCCHCo$_2$(CO)$_6$ has also furnished some surprises. The reaction of the organocobalt carboxylic acid with copper(II) methoxide leads to the copper(I) decarboxylated cluster Cu$_3${μ_2-CCHCo$_2$(CO)$_6$}$_3$,[6] instead of the expected tetracarboxylate Cu$_2${OOCCCHCo$_2$(CO)$_6$}$_4$, reminding us of the decarboxylating ability of the copper(I) salts over activated organic acids.[7] The electronic structure of the cuprous cluster shows some important degree of interaction between the copper and cobalt subsystems, which has been proposed to be the cause for the "activated" behavior of the organometallic acid.[6]

In this work we present the synthesis and properties of four new cluster of clusters molecules, the compounds Mo$_2$-{OOCCCHCo$_2$(CO)$_6$}$_4$(1,4-xylene)$_2$ (**1a**), [Mo$_2${OOCCCHCo$_2$-(CO)$_6$}$_4$(μ_2-η^6-Ar)]$_n$·*n*(1,4-xylene) (where Ar = 1,4-xylene (**1b**), toluene (**1c**)), and Cu$_2${OOCCCHCo$_2$(CO)$_6$}$_4$(H$_2$O)$_2$ (**2**). We discuss the physical properties of all the molecules on the basis of their respective electronic structures, which have been calculated by means of theoretical tools, and the effect of the organometallic −CCHCo$_2$(CO)$_6$ group on such properties. We also describe the nature of the core Mo$_2$ carboxylate and the axial arene (Ar = toluene, 1,4-xylene) and the influence of the polarity of the surroundings in this respect.

* To whom correspondence should be addressed. E-mail: vcalvo@uchile.cl. Tel: (56) 02 9782863. Fax: (56) 02 7378920.
† Universidad de Chile.
‡ Universidad de Tarapacá.

(1) (a) Clerac, R.; Cotton, F. A.; Dunbar, K. R.; Murillo, C. A.; Wang, X. *Inorg. Chem.* **2001**, *40*, 420. (b) Cotton, F. A.; Donahue, J. P.; Lin, C.; Murillo, C. A. *Inorg. Chem.* **2001**, *40*, 1234. (c) Siewers, G. F.; Malafetse, T. *J. Chem. Rev.* **2000**, *100*, 853. (d) Moreno, Y.; Vega, A.; Ushak, S.; Baggio, R.; Peña, O.; Pivan, J.-Y.; Spodine, E. *J. Mater. Chem.* **2003**, *13*, 2381. (e) McGlinchey, M. J.; Girard, L.; Ruffolo, R. *Coord. Chem. Rev.***1995**, *143*, 331.

(2) Fehlner, T. P.; Calvo-Pérez, V.; Cen, W. *J. Electron Spectrosc.* **1993**, *66*, 29.

(3) Cen, W.; Lindenfeld, P.; Fehlner, T. P. *J. Am. Chem. Soc.* **1992**, *114*, 5451.

(4) Calvo, V.; Vega, A.; Cortés, P.; Spodine, E. *Inorg. Chim. Acta* **2002**, *333*, 15.

(5) Vega, A.; Calvo, V.; Manzur, J.; Spodine, E.; Saillard, J.-Y. *Inorg. Chem.* **2002**, *41*, 5382.

(6) Vega, A.; Calvo, V.; Spodine, E.; Zárate, A.; Fuenzalida, V.; Saillard, J.-Y. *Inorg. Chem.* ***2002***, *41*, 3389.

(7) (a) Darensbourg, D. J.; Holtcamp, M. W.; Khandelwal, B.; Reibenspies, J. H. *Inorg. Chem.* **1994**, *33*, 531. (b) Toussaint, O.; Capdevielle, P.; Maumy, M. *Tetrahedron Lett.* **1987**, *28*, 539. (c) Darensbourg, D. J.; Longridge, E. M.; Atnip, E. V.; Reibenspies, J. H. *Inorg. Chem.* **1992**, *31*, 3951. (d) Darensbourg, D. J.; Longridge, E. M.; Holtcamp, M. W.; Klausmeyer, K. K.; Reibenspies, J. H. *J. Am. Chem. Soc.* **1993**, *115*, 8839.

Scheme 1

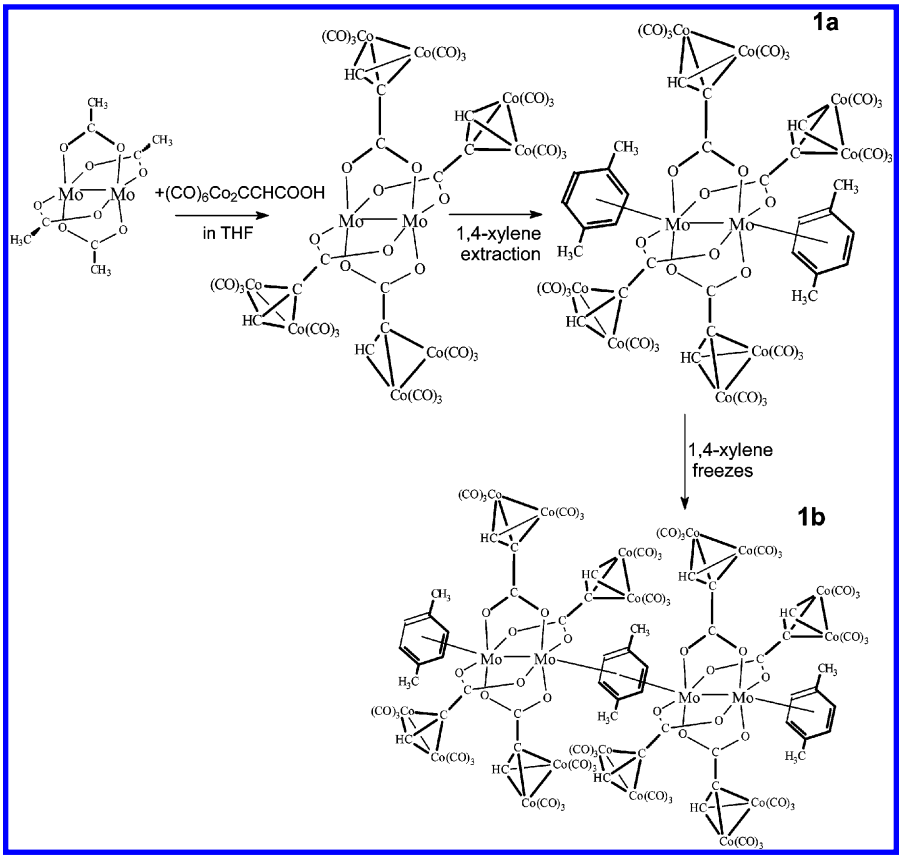

Results and Discussion

Preparation of Clusters. The mixture of molybdenum acetate (or copper acetate) and the cobalt cluster ligand in THF solution itself remains in equilibrium at room temperature (25 °C; see Scheme 1)

$$Mo_2(OOCCH_3)_4 + 4(CO)_6Co_2CCHCOOH \rightleftharpoons Mo_2\{OOCHCCCo_2(CO)_6\}_4 + 4CH_3COOH$$

unless the solution is driven to complete elimination of the acetic acid under reduced pressure:

$$Mo_2(OOCCH_3)_4 + 4(CO)_6Co_2CCHCOOH \rightarrow Mo_2\{OOCHCCCo_2(CO)_6\}_4 + 4CH_3COOH\uparrow$$

Surprisingly the products (**1b**,**c** and **2**) are very soluble in aromatic solvents; therefore we aim to understand this phenomenon. Despite the fact that the same workup was used for both clusters, the clusters of copper and molybdenum crystallize with different axial ligands. A concentrated solution of $Mo_2\{OOCHCCCo_2(CO)_6\}_4$ in toluene afforded the isolation of large needles of pillared $[Mo_2\{OOCHCCCo_2(CO)_6\}_4(toluene)]_n$ (**1c**) upon cooling to −10 °C. Crystals of this compound obtained from toluene quickly lose solvent. Crystallization of **1** in 1,4-xylene also yield long fine needles; however, as the solvent freezes a concentrated solution at the bottom of the Schlenk tube afforded the isolation of these clusters as pillars **1b**. The 1,4-xylene solvate is stable enough to allow a complete data collection. All the subsequent structural discussion is related, unless noted, to the 1,4-xylene solvate.

Structural Details. The structure of the title compound **1b** is shown in Figure 1 (bottom). Four cluster ligands $OOCCCHCo_2(CO)_6$ bridge two molybdenum centers in a syn,syn configuration. This centrosymmetric arrangement is also found in several other dimolybdenum carboxylates,[17] with an inversion center between the molybdenum atoms. The Mo−Mo distance (ca. 2.0988(9) Å) is characteristic of a quadruple Mo−Mo bond, as described in dimolybdenum(II) tetrapivalates.[18] Table 2 shows selected bond distances and angles for **1b**.

The organometallic carboxylate group $OOCCCHCo_2(CO)_6$ has the elongated pseudo-tetrahedral Co_2C_2 core also found in $Re_2\{OOCCCHCo_2(CO)_6\}_4Cl_2$.[5] The Co_2C_2 core carbon atoms of the cluster tetrahedron in **1b** are separated on average by 1.333 Å, compared to 1.342 Å measured for the dirhenium cluster.[5] The carboxylate plane O1−C1−O2 is almost coplanar

(8) Santure, D. J.; Sattelberger, A. P. *Inorg. Synth.* **1989**, *26*, 219.
(9) SHELXTL, version 5.1; Bruker AXS, Madison, WI, 1998.
(10) SMART-APEX Area Detector System; Bruker AXS, Madison, WI, 1998.
(11) SAINTPLUS, version 6.02; Bruker AXS, Madison, WI, 1999.
(12) (a) Baerends, E. J.; Ellis, D. E.; Ros, P. *Chem. Phys.* **1973**, *2*, 41. (b) Baerends, E. J.; Ros, P. *Int. J. Quantum Chem.* **1978**, *S12*, 169. (c) Boerrigter, P. M.; te Velde, G.; Baerends, E. J. *Int. J. Quantum Chem.* **1988**, *33*, 87. (d) te Velde, G.; Baerends, E. J. *J. Comput. Phys.* **1992**, *99*, 84.
(13) Amsterdam Density Functional (ADF) Program, Release 2002.01; Vrije Universiteit, Amsterdam, The Netherlands, 2002.
(14) Vosko, S. D.; Wilk, L.; Nusair, M. *Can. J. Chem.* **1990**, *58*, 1200.
(15) (a) Becke, A. D. *J. Chem. Phys.* **1986**, *84*, 4524. (b) Becke, A. D. *Phys. Rev. A* **1988**, *38*, 2098.
(16) (a) Lee, C.; Yang, W.; Parr, R. G. *Phys. Rev. B* **1988**, *37*, 785. (b) Johnson, B. G.; Gill, P. M. W.; Pople, J. A. *J. Chem. Phys.* **1993**, *98*, 5612. (c) Russo, T. V.; Martin, R. L.; Hay, P. J. *J. Chem. Phys.* **1994**, *101*, 7729. (d) Bandyopadhyay, P.; Gordon, M. S. *J. Chem. Phys.* **2000**, *113*, 1104. (e) Schmidt, M. W.; Baldridge, K. K.; Boatz, J. A.; Elbert, S. T.; Gordon, M. S.; Jensen, J. H.; Koseki, S.; Matsunaga, N.; Nguyen, K. A.: Su, S. J.; Windus, T. L.; Dupuis, M.; Montgomery, J. A. *J. Comput. Chem.* **1993**, *14*, 1347.
(17) Cotton, F. A.; Walton, R. A. *Multiple Bonds Between Metal Atoms*; Oxford University Press: New York, 1993.
(18) Cayton, R. H.; Chisholm, M. H.; Huffman, J. C.; Lobkovsky, E. B. *J. Am. Chem. Soc.* **1991**, *113*, 8709.

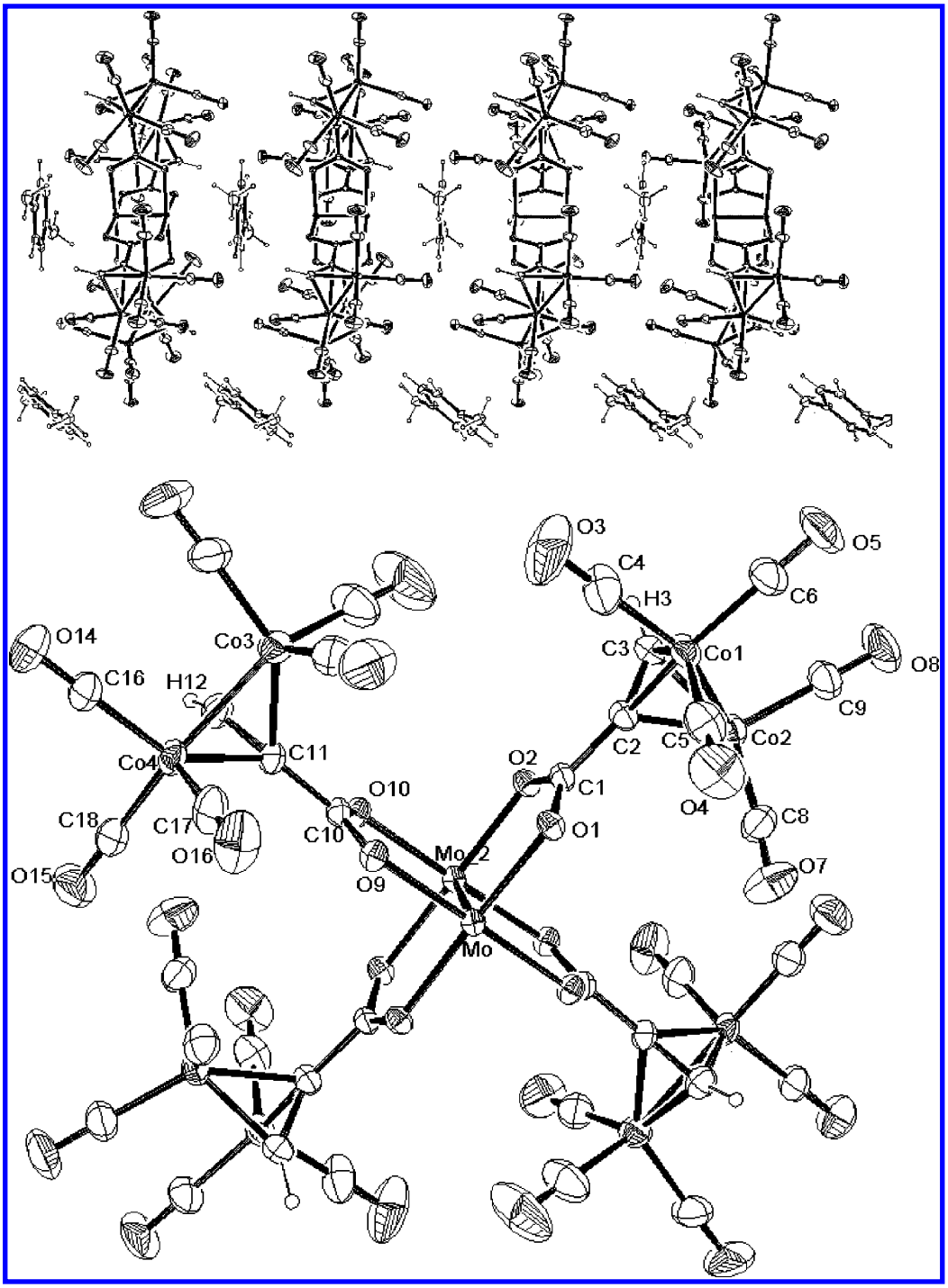

Figure 1. (Bottom) Molecular structure diagram for **1** showing a partial atomic-numbering scheme. Displacement ellipsoids are plotted at the 30% probability level, and hydrogen atoms are shown as small spheres of arbitrary radii. (Top) Packing diagram showing the 1,4-xylene···$Mo_2[OOCR]_4$···1,4-xylene pillars for **1b** at the 10% probability level.

with the plane defined by C3−C2−C1, as opposed to the situation found in the dirhenium cluster, where the average torsion angle is 50°.[5] Parallel to the MoO_4 plane at about 3.1 Å lies a 1,4-xylene molecule, as shown by the packing structure. The aromatic ring is "stacked" between two adjacent $Mo_2\{OOCHCCo_2(CO)_6\}_4$ units, in such a way as to define a linear $Mo_2\{OOCR\}_4$···1,4-xylene···$Mo_2\{OOCR\}_4$···pillar (see Figure 1, top) parallel to [100]. The methyl groups in the 1,4-xylene rings are oriented between two adjacent carboxylate planes, as shown in Chart 1a, whereas in the toluene solvate of **1c**, the methyl group of the aromatic fragment is disordered over the four available positions between the carboxylates, as shown in Chart 1b. The overall connectivity observed for toluene solvate **1c** is the same as that found for the 1,4-xylene solvate **1b**, with a Mo−Mo distance of 2.102(3) Å.

The Mo−Mo bond is not elongated in the vicinity of 1,4-xylene, as compared to the case for dichromium(II) tetrakis(carboxylate), where the axial aromatic ring seems to elongate the Cr−Cr distance as a function of the ligand basicity.[19] Chromium(II) is known to form one-dimensional arrays with substituted benzene, whose topologies are similar to those of

(19) Cotton, F. A.; Daniels, L. M.; Kibala, P. A. *Inorg. Chem.* **1992**, *31*, 1865.

Table 1. Summary of Crystal Data and Refinement Details for $Mo_2[OOCCCHCo_2(CO)_6]_4 \cdot 2(1,4\text{-xylene})$ (1b) and $Cu_2[OOCCCHCo_2(CO)_6]_4(H_2O)_2$ (2)

	1b	2
formula	$C_{52}H_{24}Co_8Mo_2O_{32}$	$C_{36}H_8Co_8Cu_2O_{34}$
formula wt	1824.03	1582.94
cryst syst	triclinic	triclinic
space group	$P\bar{1}$	$P\bar{1}$
a, Å	8.296(3)	7.705(3)
b, Å	14.247(4)	13.430(5)
c, Å	16.108(5)	13.950(5)
α, deg	114.97(2)	69.724(5)
β, deg	92.02(3)	80.724(6)
γ, deg	105.00(2)	79.883(6)
V, Å^3	1644.2(8)	1325.2(8)
Z	1	1
D_c, Mg m^{-3}	1.842	1.984
F(000)	892	770
μ(Mo Kα), mm^{-1}	2.417	3.318
R^a	0.0346	0.0721
$R_w{}^b$	0.0841	0.1624

[a] $R = \sum||F_o| - |F_c||/\sum|F_o|$. [b] $R_w = [\sum[w(F_o^2 - F_c^2)^2]/\sum[w(F_o^2)^2]]^{1/2}$. $T = 25$ °C.

Table 2. Selected Bond Distances (Å) and Angles (deg) for $Mo_2[OOCCCHCo_2(CO)_6]_4 \cdot$(1,4-xylene) (1b) and $Cu_2[OOCCCHCo_2(CO)_6]_4(H_2O)_2$ (2)

1b[a]		2[b]	
Mo−O1	2.105(3)	Cu−O1	1.975(13)
Mo−O2a	2.094(3)	Cu−O2a	1.902(13)
Mo−O10	2.113(2)	Cu−O10	1.960(14)
Mo−O11a	2.106(3)	Cu−O11a	1.945(15)
Mo−Moa	2.099(1)	Cu···Cua	2.631(5)
C1−O1	1.260(4)	C1−O1	1.294(19)
C1−O2	1.281(4)	C1−O2	1.34(2)
C10−O10	1.272(4)	C10−O10	1.25(2)
C10−O11	1.271(4)	C10−O11	1.21(2)
C1−C2	1.458(5)	C1−C2	1.550(10)
C2−C3	1.337(6)	C2−C3	1.29(3)
C10−C11	1.468(5)	C10−C11	1.51(3)
C11−C12	1.328(6)	C11−C12	1.36(2)
Co1−Co2	2.473(1)	Co1−Co2	2.471(5)
Co3−Co4	2.466(2)	Co3−Co4	2.452(5)
Mo···C20	3.326(5)	Cu−O1w	2.163(12)
Mo···C21	3.411(5)	Mo···C22	3.301(5)
Mo1···Mo1b	6.202(2)		
O1−Mo−O10	89.5(1)	O1−Cu−O10	86.6(6)
O1−Mo−O11a	90.3(1)	O1−Cu−O11a	89.2(6)
O10−Mo2−O2a	90.6(1)	O10−Cu−O2a	92.6(6)
O2a−Mo−O11a	89.4(1)	O2a−Cua−O11a	89.0(6)
O1−Mo2−O2a	176.4(1)	O1−Cu−O2a	168.9(5)
O10−Mo−O11a	176.3(1)	O10−Cu−O11a	166.9(5)
O1−C1−O2	122.8(3)	O1−Cu−O1w	97.7(5)
C1−C2−C3	143.8(4)	O10−Cu−O1w	102.2(5)
O10−C10−O11	122.9(3)	O2a−Cu−O1w	93.3(5)
C10−C11−C12	140.9(4)	O11a−Cu−O1w	90.7(5)
Moa−Mo···Mob	175.37(2)	O1−C1−O2	119(2)
O10−C10−O11	127(2)	C1−C2−C3	142(2)
		C10−C11−C12	138(2)

[a] Symmetry transformations: (a) $-x + 1, -y, -z + 1$; (b) $-x, -y, 1 - z$. [b] Symmetry transformation: (a) $-x, -y + 1, -z$.

Chart 1

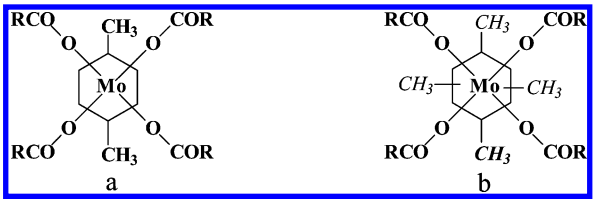

Rh(II) tetrakis(trifluoroacetate).[20] While bis(benzene)chromium-(0)[21] is a mononuclear arene with a short Cr−C distance, the related arenes of Sc(0), Ti(0), and V(0) form multidecker arrays,

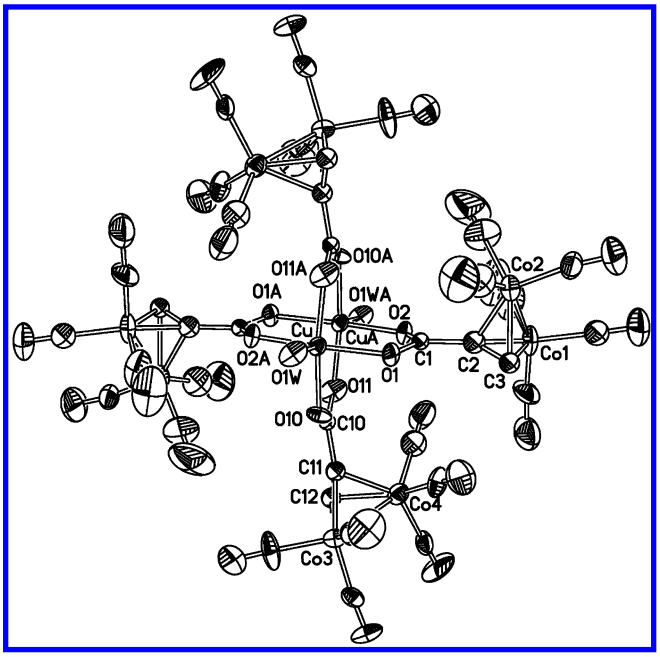

Figure 2. Molecular structure diagram for **2** showing a partial atomic-numbering scheme. Displacement ellipsoids are plotted at the 33% probability level, and hydrogen atoms are shown as small spheres of arbitrary radii.

where the negative potential on the arene points to an electronically unsaturated metal,[22] as in **1b**. A considerable body of structural evidence shows that the low-oxidation-state species $M_2[OOCR]_4$ (where M = Cr(II),[19] Mo(II),[23] Rh(II)[20]) can be packed with aromatic compounds through the axial positions of the metal centers. These noninnocent aromatic solvents, such as 1,4-xylene, have been reported to coordinate to the axial positions of dichromium tetracarboxylates, where the aromatic ring is stacked in an η^6 fashion between two adjacent Cr^{II}_2 centers, forming a chain or pillar.[19] Numerous difficulties in obtaining crystals suitable for X-ray diffraction arise from the disorder found in the substituted arene in dichromium carboxylates and the freezing point of the solvent. The Cr(II)···arene distances reported for $Cr_2(OOCCPh_3)_4(1,4\text{-xylene})_2$ are 3.310 Å, with an elongated Cr−Cr core (2.291 Å), while in $Cr_2(OOCCPh_3)_4$-(1,4-difluorobenzene)$_2$ the arene is 3.388 Å away from the metal. Interestingly, this complex exhibits a shorter Cr−Cr distance (2.176 Å), where the Cr−Cr distance seems to correlate to the donor ability of the arene. We were unable to observe Mo−Mo bond lengthening upon stacking of the 1,4-xylene, which is indicative of the nature of the pillar formation.

Figure 2 shows a molecular diagram of the complex $Cu_2\{OOCCCHCo_2(CO)_6\}_4(H_2O)_2$ (**2**). Table 2 gives some bond distances and angles and torsion angles for **2**. This complex has a copper acetate dimer structure, with four carboxylate groups bridging the cupric centers and two water molecules as terminal axial ligands. The inversion center of the space group $P\bar{1}$ coincides with the midpoint of the copper−copper distance, defining C_i as the molecular symmetry group. The copper−copper distance is 2.636(6) Å, a normal value for copper

(20) Cotton, F. A.; Dikarev, E. V.; Petrukhina, M. A. *J. Am. Chem. Soc.* **2001**, *123*, 11655.
(21) Seyferth, D. *Organometallics* **2002**, *21*, 2800.
(22) (a) Kurikawa, T.; Takeda, H.; Hirano, M.; Judai, K.; Arita, T.; Nagao, S.; Nakajima, A.; Kaya, K. *Organometallics* **1999**, *18*, 1430. (b) Yasuike, T.; Yabushita, S. *J. Phys. Chem. A* **1999**, *103*, 4533.
(23) Campanci, C.; Dunbar, K. R.; Ouyang, X. *J. Chem. Soc., Chem. Commun.* **1996**, *21*, 2427.

carboxylate dimers and very similar to the value reported for copper acetate, 2.619 Å.[24]

The average cobalt−cobalt distance (2.467 Å) in the four carboxylate ligands is shorter than the measured value in the free carboxylic acid, 2.483(3) Å.[4] In the same way, the carboxylate fragment torsion angle (defined by O−C−C−C) has an average value of 34°, which is smaller than the average value measured for $Re_2\{OOCCCHCo_2(CO)_6\}_4Cl_2$ (50°), for $HOOCCCHCo_2(CO)_6$ (94°), and, of course, for **1b** (∼0°). It is likely that this torsion angle is defined by packing and/or steric factors, and it may play an important role in the electronic communicating ability of the propiolic fragment.[4]

Cyclic Voltammetry. Both molecules, **1** and **2**, have two electroactive sites, namely the central M_2 core and the peripheral $Co_2(CO)_6$ fragments; therefore, signals arising from both can be expected. The observed CV for **1** in CH_2Cl_2 (DCM) has an oxidation peak at +750 mV, with a corresponding reduction at +617 mV. The measured $i_{p,a}/i_{p,c}$ ratio of 0.73 indicates a quasi-reversible oxidation, which can be attributed to the Mo_2 center. This signal ($E_{1/2}$ = −694 mV) is significantly shifted when compared to the Mo(II) oxidation value in $Mo_2(OOCCH_3)_4$ ($E_{1/2}$ = −450 mV).[25] The voltammogram also shows an irreversible reduction wave at −1076 mV, which can be assigned to the $CCCo_2(CO)_6$ fragments. The rapid decomposition of $Cu_2\{OOCCCHCo_2(CO)_6\}_4(H_2O)_2$ prevents the electrochemical measurements in CH_2Cl_2, where the electrochemical behavior of the parent ligand has been described. Since a change in the solvent to acetone hardly affects the shape and position of the voltammogram of the ligand, we have recorded the voltammogram of **2** in this solvent. It shows two electrochemical signals, but differing from the case for **1**, as in **2** they correspond to two completely irreversible reductions at $E_{p,c}$ = −684 mV and $E_{p,c}$ = −976 mV. The last reduction is quite comparable to the reduction potential measured for $HOOCCCHCo_2(CO)_6$ in acetone, $E_{p,c}$ = −926 mV, suggesting that this reduction is related to the $-Co_2(CO)_6$ core. The measured value for $HOOCCCHCo_2(CO)_6$ in CH_2Cl_2 is −1015 mV.[4] The reduction wave observed at −684 mV can be attributed to the two-electron reduction of the Cu_2 central core, considering that a copper(II) monomer carboxylate would be reduced at about −370 mV.[26] No metallic copper oxidation wave was observed in the oxidation sweeps, suggesting that the copper reduction step does not reach metallic copper at the attained potentials. The measured reduction potential suggests very stabilized copper(II) centers.

The shifts of the potentials for the reduction and/or oxidation of the signals on the clusters, relative to those of the copper acetate (or molybdenum acetate), clearly suggest that both dicopper and dimolybdenum cores transfer some electron density to the cobalt carbonyl ligand through the carboxylate bridge, and both electroactive centers can be considered as mutually connected.

Computational Methods. On the basis of their XAlfa SW results[19] on the $Cr_2(OOCCPh_3)_4\cdots$(arene) system, Cotton et al. postulated an electron donation from the arene (π orbital) to Cr−Cr (π^* orbitals) to explain the elongation of the Cr−Cr bond. Cotton's recent EH interpretation of the packing of $Rh_2(OOCCF_3)_4\cdots$(arene) led him to conclude that high-electron-density centers on the arene are preferred sites for η^1 binding to the dirhodium trifluoroacetate, "a Lewis acid".[20] In addition, 1,3-xylene has been reported to approach in an η^2 fashion to a dimolybdenum trifluoroacetate within a complex scaffolding of TCNQ.[23] The 1,3-xylene molecules of dimolybdenum carboxylates were found to be entangled by TCNQ to the neighbor molecules of $Mo_2(OOCCF_3)_4$, but the 1,3-xylene sits far from the Mo−Mo center. This situation has been classified as enclathration by the authors. The currently observed $Mo_2\{OOCCCHCo_2(CO)_6\}_4\cdots$(1,4-xylene) interaction in the cluster of clusters **1** can be considered as a challenge, since the negative electronic potential of the molybdenum−oxo fragment point toward the 1,4-xylene faces, as shown in the synopsis.

The cluster was modeled using double-ζ basis functions and toluene as PCM, reproducing the Mo−Mo, Mo−O, and O−C distances within 0.03 Å. The single-point DFT results on a supermolecule ((arene)$\cdots Mo_2(RCOO)_4\cdots$(arene)) indicate that the molybdenum δ orbital hardly combines with the benzene orbitals, owing to the low overlap (0.0002) existing with the π system of the arene. However, molybdenum π orbitals (E) show a more pronounced overlap (0.047) with the filled aromatic π^* (E symmetry). Therefore, our calculations are oriented to determine the perturbation of a first solvation sphere (effective fragment potential) and a second sphere of solvation (polarizable continuum media). In an excellent recent review Tomasi compiled a broad spectrum of applications of this computational method.[27] The PCM method calculates the free energy (ΔG_{solv}) required to bring one molecule of solute from the gas phase to a polarizable dielectric media. This requires opening a cavity in the solvent where the solute can be fitted (ΔG_{cav}), and therefore, some steric repulsions arise (ΔG_{rep}); van der Waals contributions to the energy of this process are included as ΔG_{disp}, but more importantly, the electrostatic stabilization due to the dielectric, ΔG_{eletr}, is solved self-consistently with the solute wave function. The last contribution greatly relaxes the solute in the solvent:

$$\Delta G_{solv} = \Delta G_{cav} + \Delta G_{rep} + \Delta G_{eletr} + \Delta G_{disp}$$

On the other hand, the effective fragment potential method calculates the energy of the solute surrounded by point charges of discrete molecules of solvent (benzene or 1,4-xylene). In a previous run one calculates the electric dipoles, quadrupoles, and multipoles of a single solvent molecule and then one recalculates ab initio the effect of these electric charges on the solute−solvent array.

Our DFT results on the optimized cluster **1** agree with previous assumptions on the nature of the electronic spectra, as a metal (Mo_2) to ligand ($Co_3(CO)_9$) charge transfer.[2,28a] A single-point calculation based on the optimized geometry shows that the highest occupied frontier orbital is a δ symmetry orbital (87% Mo_2 character in **1**), while the LUMO and nearby virtual orbitals have $Co_2CC(\sigma^*)$ symmetry. The observed bathochromic shift of the MLCT with increasing solvent polarity in the visible spectra of **1** also agrees with the MLCT nature of this transition.[28b] DFT calculations of this Mo(II) cluster **1** in three polarizable continuum media (PCM) indicate a net stabilizing effect of the Coulomb contribution on the solvent free energy, while the formation of the cavity is a destabilizing factor. The stabilizing effect is more pronounced on the filled orbitals. As a result, the energy gap between the LUMO and the δ character orbital is larger in methylene chloride than in THF, as shown in Table 3, which explains the bathochromic effect of the solvent.

(24) (a) Van Niekerk, J. N.; Schoening, F. R. *Acta Crystallogr.* **1953**, *6*, 227. (b) de Meester, P.; Fletcher, S. R.; Skapski, A. C. *J. Chem. Soc., Dalton Trans.* **1973**, 2575.
(25) Cotton, F. A.; Lin, C.; Murillo, C. A. *Inorg. Chem.* **2001**, *40*, 478.
(26) Koo, B. K. *Bull. Korean Chem. Soc.* **2001**, *22*, 113.
(27) Tomasi, J.; Mennucci, B.; Cammi, R. *Chem. Rev.* **2005**, *105*, 2999.
(28) (a) Calvo-Pérez, V. F.; Fehlner, T. P.; Rheingold, A. R. L. *Inorg. Chem.* **1996**, *35*, 7289. (b) Glöcklea, M.; Katzb, N. E.; Ketterlea, M.; Kaima, W. *Inorg. Chim. Acta* **2002**, *336*, 55.

Table 3. Free Energy Changes of ΔG_{solv} of $Mo_2[OOCCCHCo_2(CO)_6]_4$ (1b) Going from the Gas Phase to the Solution, As Calculated by PCM[a]

solvent	calcd $\Delta\Delta G_{solv}$ (kcal/mol)	calcd gap (10^{-4} cm^{-1})	exptl E_{vis} (10^{-4} cm^{-1})
CH_2Cl_2	−45.10	7.54	17.15
$CH_3C_6H_5$	−8.43	7.49	16.63
C_4H_8O	26.0	7.26	15.26

[a] Gap of energy between LUMO and the filled δ MO as compared to the observed energy of the transition in the visible region (E_{vis}). A diagram of the experimental results in these solvents is included in the Supporting Information.

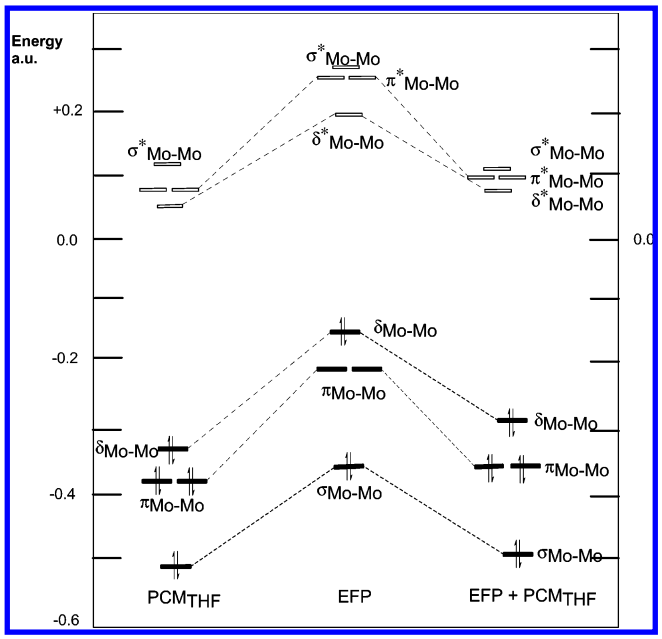

Figure 3. Orbital diagram for the model compound $Mo_2(OOCH)_4$ optimized with toluene as PCM (left), in the presence of two benzene fragment potentials (EFP; middle), and in the presence of a benzene effective fragment potential and a continuum polarizable (EFP+PCM; right).

Going further into the nature of the molybdenum−arene interaction, we constructed a model where two benzene (or two 1,4-xylene) effective fragment potentials surround the $Mo_2\{OOCH\}_4$ unit, as a way to test the effect of the potential of the aromatic ring on the dimolybdenum center. The EFP calculation (ab initio, non-DFT) on the optimized carboxylate $\{Mo_2(OOCH)_4\}$ was also done in the presence of a polarizable continuum media (toluene). Both EFP results indicate that the benzene fragment polarizes the Mo−Mo axis (+0.019 D) and redistributes the negative charge over the O−Mo−O planes. The resulting energies of the model compound with EFP and EFP+PCM are shown in Figure 3. The empty and filled orbitals are destabilized in the presence of the arene multipoles and are stabilized in the presence of a polarizable continuum media. These calculations are consistent with EHMO calculations on the dirhodium trifluoroacetates, which suggest that the aromatic systems act as Lewis bases and the metal−metal manifold accepts the electron density.[20]

The inclusion of a toluene polarizable continuum around $Mo_2(OOCCCHCo_2(CO)_6)_4$ shows the same trend found using density functional theory on the optimized $Mo_2(OOCH)_4$, which indicates a moderate electrostatic stabilization and a large destabilizing cavitation free energy. Further computational details are included as Supporting Information.

$Cu_2\{OOCCCHCo_2(CO)_6\}_4(H_2O)_2$. Although it is clear that the value for $-2J$ in the copper(II) carboxylate dimers $Cu_2[OOCR]_4(H_2O)_2$ does not correlate with the copper−copper distance or the electronegativity of the R substituent group,[29] there is clear evidence of the electronic effect of the nature of R on $-2J$.[30] In the case of R = $CCHCo_2(CO)_6$, where the magnetic contribution is diluted over an important amount of diamagnetic fragments, the magnetic response of the copper(II) dimer is different from that observed for simple copper(II) carboxylates such as acetate, which is known to be antiferromagnetically coupled.

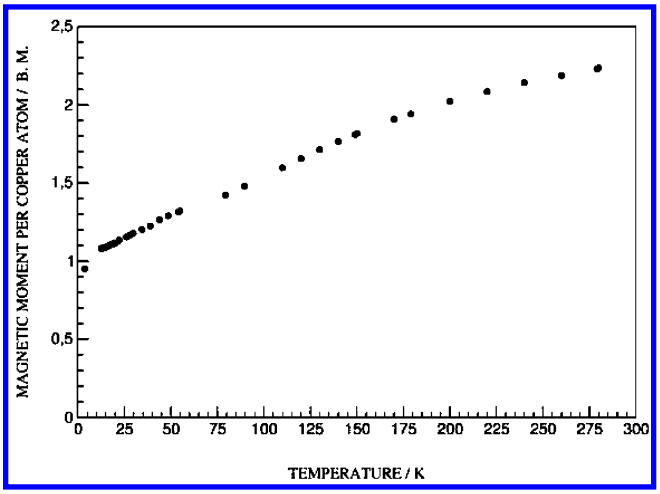

Figure 4. Temperature dependence of the magnetic moment per copper atom for compound **2**.

The temperature dependence of the effective magnetic moment per copper atom for **2** steadily decreases from 2.2 μ_B to about 1.0 μ_B from room temperature to 9 K (see Figure 4), suggesting some kind of antiferromagnetic coupling between the cupric centers. The efforts to fit the curve to the Bleaney−Bowers equation for $S = {}^1/_2$ coupled dimers were unsuccessful. Since there are no great structural differences between **2** and other copper(II) carboxylates (i.e. acetate) which could explain the failure to fit the curve to the Bleaney−Bowers equation, we used modern DFT theoretical methods to evaluate the coupling constant. These have been successfully used on a variety of copper dimers[31] to explain the observed magnetic coupling phenomena. The $-2J$ value was directly computed as the difference between the broken-symmetry singlet ($E_{S=0}$) and the triplet state ($E_{S=1}$), as proposed by Ruiz et al.[31] This difference for **2** is 363 cm^{-1}, while the described value for copper acetate at the same level of approximation is about 8000 cm^{-1}. Since both compounds have similar central $Cu_2\{OOCR\}_4(H_2O)_2$ motifs, the difference can be ascribed to the electronic properties of the cluster carboxylate ligand. Despite the lack of accuracy of this level of calculation, the difference of 1 order of magnitude between copper acetate and **2** clearly suggests that this cluster of clusters is a very weak antiferromagnet.

Conclusions. We have demonstrated experimentally that electronic transitions of the Mo(II)−$OOCCCHCo_2(CO)_6$ clusters can be attributed to a MLCT, as indicated by its dependence on the nature of the solvent. In addition, according to our calculations, electron donation occurs from the arene π system to the dimolybdenum π^* manifold in $Mo_2\{OOCR\}_4\cdots(Ar)$ in the ground state. 1,4-Xylene seems to stabilize the $Mo_2\{OOCR\}_4$ cluster by about 8 kcal mol^{-1}, and the whole pillared cluster is

(29) Moreland, J. A.; Doedens, R. J. *Inorg. Chem.* **1978**, *17*, 674.
(30) Steward, O. W.; McAfee, R. C.; Chang, S.-C.; Piskor, S. R.; Schreiber, W. J.; Jury, C. F.; Taylor, C. F.; Pletcher, J. F.; Chen, C.-S. *Inorg. Chem.* **1986**, *25*, 771.
(31) Ruiz, E.; Cano, J.; Alvarez, S.; Alemany, P. *J. Am. Chem. Soc.* **1998**, *120*, 11122.

still a favored structure. The particular topology of the cluster of clusters chain $Mo_2(OOCHCCCo_2(CO)_6)_4$ is determined by the topology of 1,4-xylene and the polarity of the environment. In the same way, the electronic nature of R = $OOCCCCo_2(CO)_6$ strongly modifies the coupling constant in the copper(II) cluster of clusters dimer compared to the case for copper(II) acetate. Interestingly, in spite of the fact that the synthetic workup was the same for Mo(II) and Cu(II) clusters, the copper(II) cluster presents the oxo ligands in axial positions, while molybdenum(II) prefers the arene ligands. This synthetic approach allows us to assemble heterometallic clusters with several Mo/Co ratios in order to design new metallic materials.

Experimental Section

All manipulations were carried out under a argon atmosphere using standard Schlenk techniques. All solvents were dried under nitrogen using standard drying agents. Dicobalt octacarbonyl, $Co_2(CO)_8$, was purchased from Fluka. Propynoic acid (propiolic acid) was purchased from Aldrich and used without further purification. Molybdenum(II) acetate was prepared from $Mo(CO)_6$ (Alfa), which was reacted with acetic acid/acetic anhydride according to Santure's method.[8] All the solvents used were distilled and dried under argon just before the preparation and all the manipulations (unless stated) were carried out under an inert atmosphere using standard Schlenk techniques. Electronic spectra were measured on a UNICAM-UV3 spectrometer, under an inert atmosphere. FTIR spectra were recorded on a Bruker IFS 28 spectrometer.

Syntheses. Procedure for Preparation of the Cluster Ligand $(CO)_6Co_2HCCCOOH$. The cluster carboxylic acid $(CO)_6Co_2HCCCOOH$ was obtained by reaction of dicobalt octacarbonyl and propiolic acid (HCCCOOH) as described,[4] with the following modifications: the raw solution was concentrated under reduced pressure until an orange solid crystallized. The solid that was filtered off was dissolved in methanol. Half the volume of 2 M HCl was added to the cold methanol solution and the resulting solution allowed to evaporate slowly. This procedure yields 60% of the cluster carboxylate and a pink aqueous solution ($CoCl_2$). The product was identified by FTIR and elemental analyses as reported before.

General Procedure for the Synthesis of 1. Method A. 1a. A 200 mg amount of the cluster ligand $(CO)_6Co_2HCCCOOH$ was reacted with 60 mg of dimolybdenum(II) tetraacetate in 5 mL of THF over 1 h at room temperature. A dark green solution quickly develops at room temperature, just after mixing the reagents with magnetic stirring. The resulting deep green solution was dried under vacuum and then extracted with 10 mL of warm 1,4-xylene. The solid was dispersed with an ultrasonic bath, with warming to 50 °C, and then the solution was filtered through silica. The 1,4-xylene solution was concentrated to half the volume and left in the dark at 15 °C for 1 day. The next day, the solution was cooled to 10 °C for 1 week. A large portion of the solvent sublimed above the green concentrate, leaving long dark green needles gathered at the bottom of the tube in a concentrated solution. After the Schlenk tube was thawed, some 50 mg of dark green needles were filtered out for analyses. The yield of **1a** was 64% based on $Mo_2(OOCCH_3)_4$. Compound **1a** was characterized by elemental analysis and FTIR and ^{1}H NMR spectroscopy. IR (KBr): 2103 m, 2065 s, 2027 s, 1544 m, 1475 w, 1478 m, 1428 m, 1327 m, 723 m cm^{-1}. Anal. Calcd for $Mo_2(C_9Co_2O_8H)_4(C_8H_{10})_2$: C, 34.65; H, 1.37; Co, 25.66; Mo, 10.44. Found: C, 33.96; H, 0.75; Co, 26.36; Mo, 11.41. ^{1}H NMR (300 MHz, d_6-benzene): 7.250 (s, 4H), 5.410 (s, 4H), 2.290 (s, 6H).

Method B. 1b. Further recrystallization of **1a** afforded thick needles of **1b**. A single crystal used for X-ray diffraction was obtained from the concentrate at the bottom of the Schlenk tube after the 1,4-xylene froze. IR (KBr): 2103 w, 2065 s, 2027 s, 1544 m, 1475−1478 m, 1327 m, 723 m cm^{-1}. The medium-broad band appearing at 1544 cm^{-1} is assigned to the bending of the 1,4-xylene ring. Anal. Calcd for $Mo_2(C_9Co_2O_8H_4)_4(C_8H_{10})$: C, 31.21; H, 0.93. Found: C, 34.25; H, 1.29. Metal analysis by MS-ICP reveals a Co to Mo mole ration of 7.84:2.

1c. Cluster **1** can also be crystallized as a toluene solvate from a toluene solution, following the synthetic route described above. IR (KBr): 2105 w, 2067 s, 2025 s, 1552 m, 1470 m, 1326 m, 723 m cm^{-1}. The needles melt at 35 °C. Vis: in THF, 655 nm (5600 M^{-1}cm^{-1}) in CH_2Cl_2, 583 nm (1540 M^{-1} cm^{-1}); in toluene, 602 nm (5600 M^{-1}cm^{-1}).

2. Copper acetate was refluxed for 1 h in glacial acetic acid and crystallized before use to remove any basic acetate traces. It has been shown that a basic media can decarboxylate $HOOCCCHCo_2(CO)_6$.[6] A 2.81 mmol portion of $HOOCCCHCo_2(CO)_6$ dissolved in 50 mL of THF was slowly added to a THF solution of 0.70 mmol of copper(II) acetate with stirring. After 1 h of reaction, the solvent was completely evaporated under reduced pressure. The resulting black-brown solid was extracted with portions of 1,4-xylene (10 mL), until the extracting solvent became colorless. Then, the 1,4-xylene solution was filtered through activated silica. After volume reduction at reduced pressure, the solution was allowed to stand at 5 °C. The solution must be kept away from light. Plate-shaped microcrystals were obtained after 1 day. Anal. Calcd for $C_{36}H_8Co_8Cu_2O_{34}$: C, 27.3; H, 0.5; O, 34.4; Cu, 8.0; Co, 29.8. Found: Cu, 8.5; Co, 29.1 (Co:Cu = 4.0). IR (KBr): 2102 m, 2032 s (μ_{CO}), 1594 m, 1539 m, 1340 m, 722 m cm^{-1}.

X-ray Diffraction. Crystals of **1b** and **2** suitable for X-ray structural determinations were mounted on glass fibers at room temperature in a Siemens R3m diffractometer. The crystals are dichroic, with a red tint, which is observed upon rotation. Cell parameters were calculated from least-squares fitting of 25 high-angle reflections ($7.5 \leq \theta \leq 15°$). The structures were solved by means of direct methods using XS in SHELXTL[9] and completed by means of difference Fourier synthesis. Full-matrix least-squares and isotropic refinement was performed for all non-hydrogen atoms until convergence using XL in SHELXTL.[9] The acetylenic hydrogen atoms and 1,4-xylene hydrogen atoms in the title compound **1b** were located by Fourier synthesis and were not refined in subsequent least-squares cycles. Crystal data for **1b** and **2** are given in Table 1.

Magnetic Susceptibility. A 50 mg portion of crystalline $C_{36}H_8Co_8Cu_2O_{34}$ (**2**) was placed in a gelatin capsule and χ measured in a Cryogenics SQUID magnetometer from 3 K up to room temperature. The applied magnetic field was set at 0.1 T. Experimental data were corrected for diamagnetic contributions for the copper and cluster groups (-2.58×10^{-4} cm^3/mol).

Cyclic Voltammetry. All measurements were recorded in a BASi CV-50W voltammetric analyzer at various sweep rates: 50, 100, 200, 300, 400, and 500 mV s^{-1}. A vitreous-carbon electrode was used as the working electrode, a platinum electrode was used as the auxiliary electrode, and a saturated calomel electrode was used as the reference electrode. The observed voltammograms for **1** and **2** were obtained in CH_2Cl_2 (and acetone) with tetrabutylammonium hexafluorophosphate 0.1 M as supporting electrolyte.

Computational Details. The geometry optimization of cluster **1** was carried out using LANL2DZ basis functions from PNL using the B3LYP functional on the package GAMESS assuming C_4 symmetry. Single-point energy calculations of cluster **1**, a supermolecule including benzene, and model fragments were carried out using double-ζ basis functions from PNL using the B3LYP functional in the package GAMESS. Basis sets were obtained from the Extensible Computational Chemistry Environment Basis Set Database, Version 02/25/04, as developed and distributed by the Molecular Science Computing Facility, Environmental and Molecular Sciences Laboratory, which is part of the Pacific Northwest Laboratory, P.O. Box 999, Richland, WA 99352, and funded by the U.S. Department of Energy. Comparisons of EFP, PCM, and EFP+PCM [16d] were done at the Hartree−Fock level using GAMESS.[16e] DFT[12] calculations were carried out for cluster **2** using

the Amsterdam density functional (ADF) program.[13] The Vosko−Wilk−Nusair parametrization[14] was used for the local density approximation with gradient corrections for exchange (Becke88)[15] and correlation (Lee−Yang−Parr)[16a] (BLYP), respectively. The numerical integration procedure applied to the calculations was developed by te Velde.[12d] The integration factor considered for all calculations was 4.0. The frozen-core approximation was used to treat core electrons.[12d] A standard ADF TZP basis was used.

Acknowledgment. We acknowledge the FONDECYT (Grant Nos. 1980896 and 2990093) and FONDAP (Grant No. 11 98 0002) and also thank *MOLYMET S.A.* for their kind support and interest in our research on molybdenum compounds. We are grateful to "*Fundación Andes*" for the purchase of the area detector system, currently operating at the *Universidad de Chile*.

Note Added after ASAP Publication. In the version of this paper published on the Web March 9, 2005, the units for density (D_c) in Table 1 were incorrect. The units that now appear are correct.

Supporting Information Available: CIF files giving all X-ray crystallographic data, including atomic positions, thermal parameters, and bond distances and angles for **1b**,**c** and **2** in cif format and tables and figures giving optimized coordinates for the model complexes $Mo_2(OOCCCHCo_2(CO)_6)_4$, electronic spectra of cluster **1b** in three different solvents, and cyclic voltammograms for **1**. This material is available free of charge via the Internet at http://pubs.acs.org.